Journal of Applied Physics ARTICLE scitation.org/journal/jap

Post-processing method for extracting the resistivity of Rare-Earth Barium Copper Oxide (REBCO) coated conductors in over-critical current conditions from ultra-fast *V-I* pulsed current measurements

Cite as: J. Appl. Phys. **126**, 023902 (2019); doi: 10.1063/1.5095637
Submitted: 11 March 2019 · Accepted: 22 June 2019 ·
Published Online: 12 July 2019

View Online Export Citation CrossMark

S. Richard,[a] F. Sirois,[b] and C. Lacroix

AFFILIATIONS

Polytechnique Montreal, Montreal, Quebec H3C 3A7, Canada

[a]**Electronic mail:** simon.richard@polymtl.ca
[b]**Electronic mail:** f.sirois@polymtl.ca

ABSTRACT

This paper presents a simple but rigorous method to extract correctly the resistivity of the superconducting Rare-Earth Barium Copper Oxide (REBCO) layer of High Temperature Superconductor coated conductors, when the latter are characterized in over-critical current conditions using ultrafast *V-I* pulsed current measurements. The pulsed current measurement method is used to reduce the amount of heat generated by the strong current flowing in the sample, but it cannot prevent it completely at current levels well above the critical current. In order to estimate accurately the temperature rise, we developed the so-called "Uniform Current" (UC) model, which consists in a static current sharing model coupled with a 2D thermal solver. The model assumes that the electric field is uniform over the sample cross section. It has been shown that this hypothesis works fine at high currents, but for lower current levels, although still higher than the critical current, one must wait until the magnetic relaxation effects disappear before using the outputs of the UC model. We also derived a theoretical bound for the error related to magnetic relaxation, which can be estimated experimentally by using a rectangular pick-up coil located just above the sample surface. After applying the UC model on an experimental set of data, one obtains a whole set of data points defining the resistivity $\rho(J, T)$ of the REBCO superconductor being characterized.

I. INTRODUCTION

A lot of work has been done over the last few years to improve the performance of second-generation high temperature superconductor coated conductors (2G HTS CCs). These CCs (or simply "tapes") have great potential of use in many technological applications. The development of these applications greatly benefits from numerical modeling, which requires accurate material models. This is not a problem for superconductors operated below or near their critical current (I_c), but for applications in which CCs are driven above their I_c, such as fault current limiters or during pulsed field magnetization, the superconducting material enters into a highly dissipative flux flow regime, with intense heat generation and rapid temperature rise. Determining the current and temperature dependence of the resistivity above I_c is thus difficult, and for that reason, the electrical behavior of superconductors in the flux flow regime remains largely unknown.[1]

One possible solution to reduce the impact of heating during measurements above I_c is to use a pulsed current technique.[2,3] For this purpose, Sirois *et al.*[4] developed an ultrafast, high pulsed current source, which can generate square current pulses up to 1500 A with a plateau duration as short as 10 μs and a current rising rate up to 500 A/μs.[4] A typical current pulse generated with this system is shown in Fig. 1, where the basic quantities describing the pulse are defined, i.e., the time rise (t_r), the maximum current (I_{max}), and the pulse duration (t_p).

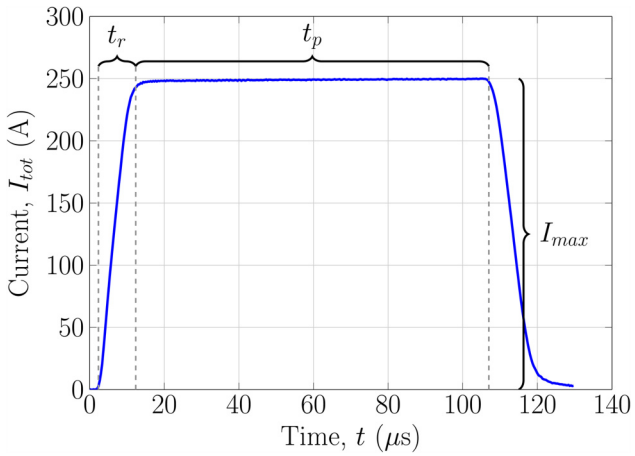

FIG. 1. Typical current pulse used for the electrical characterization of HTS coated conductors (CCs). The pulse is characterized by (i) a rise time (t_r), (ii) a current amplitude (I_{max}), and (iii) a plateau duration (t_p).

Even with ultrafast current pulses, the temperature rise in the sample cannot be systematically neglected. For instance, in Therasse *et al.*,[5] a temperature rise of 13 K (from 77 K to 90 K) was attained in less than 35 μs when a current $I_{\max} = 3I_c$ was applied in a CC with a thin silver stabilizer (2 μm). As a consequence, the current sharing between each conducting layer in the tape, i.e., the superconductor, the silver stabilizer, and the hastelloy substrate, changes as the temperature increases. This has to be taken into account in order to extract meaningful values of the superconductor resitivity ρ_{HTS} vs the instantaneous values of current density J and temperature T.

In this paper, we present a simple electrothermal model that we called "Uniform Current" (UC) model, which takes into account temperature rise and current sharing between the various conducting layers of 2G HTS CCs during a current pulse. This model allows extracting correctly the $\rho_{HTS}(J, T)$ characteristic of the superconducting material from ultrafast pulsed current measurements (on the microsecond scale) when $I_{\max} > I_c$.

The paper is organized as follows. At first, with the help of a magnetothermal model based on the H-formulation, we study in detail the dynamics of current, electric field, and voltage measurements during ultrafast current pulses. Then, we present the details of the newly developed UC model. The accuracy and conditions of the validity of the UC model are evaluated by comparing its outputs to a reference case calculated with the magnetothermal model, which involve no major physical approximation. Finally, experimental results are presented and analyzed with the help of the UC model. As a complement, a theoretical error bound for the resistivity obtained with the UC model is derived in the Appendix.

II. CURRENT AND VOLTAGE DYNAMICS DURING FAST CURRENT PULSES

A. Magnetothermal model

To study the various physical dynamics that occur during ultrafast pulsed current measurements, an electromagnetic model coupled with a thermal model is necessary. Our electromagnetic model is based on the well-known H-formulation, which can be written in 2D in its usual decoupled form (current flowing along the z axis)[6,7]

$$\mu_0 \frac{\partial H_x}{\partial t} + \frac{\partial E_z}{\partial y} = 0, \tag{1}$$

$$\mu_0 \frac{\partial H_y}{\partial t} - \frac{\partial E_z}{\partial x} = 0, \tag{2}$$

where $E_z = \rho J_z$, and J_z is given by

$$J_z = \frac{\partial H_y}{\partial x} - \frac{\partial H_x}{\partial y}. \tag{3}$$

Equations (1)–(3) are solved with the finite element method with COMSOL 4.3b, in order to obtain a solution in terms of H_x and H_y, from which we derive J_z. The 2D approximation is valid here because the voltage taps are located more than 2 cm away from the current contacts, which is longer than the current transfer length of the sample used in our experiments. The total current I_{tot} flowing in the simulated tape is imposed with the following constraint:

$$I_{tot}(t) = \iint J_z \, dx \, dy. \tag{4}$$

The thermal effects are taken into account by solving the heat diffusion equation simultaneously with the electromagnetic problem. The general form of the heat equation reads as follows:

$$c_v \frac{\partial T}{\partial t} - \nabla \cdot (\kappa \nabla T) = Q, \tag{5}$$

where κ is the thermal conductivity, c_v is the volumic specific heat, and Q represents the local heat generation. In the 2D case considered in this paper, $Q = E_z J_z$. No external cooling is applied at the boundary of the tape (the adiabatic regime), as in the pulsed current regime, the heating power generated by the pulse is systematically 2–3 orders of magnitude higher than the heat evacuated by convection. However, the addition of convective cooling can easily be implemented by adding a Neumann boundary condition to model the Newton law of cooling, such as in (5).

It is worth mentioning that the temperature profile $T(x, y)$ cannot be assumed as uniform throughout the CC cross section, and especially not across its thickness. For instance, the thermal diffusivity of hastelloy at 77 K is $D = \kappa/c_v = 4.32 \times 10^{-6}$ m^2/s.[8] Knowing that the diffusion length $\lambda = 2\sqrt{Dt}$,[9] we find that it takes more than 100 μs for heat to diffuse through a typical 50-μm-thick hastelloy substrate used in superconducting tapes. We thus conclude that the internal temperature gradient inside tapes must be taken into account when performing postprocessing on fast pulsed current measurements.

B. Coated conductor model

The geometry of the HTS CC sample considered in this paper is shown in Fig. 2 (not to scale). It consists of a 4-mm-wide

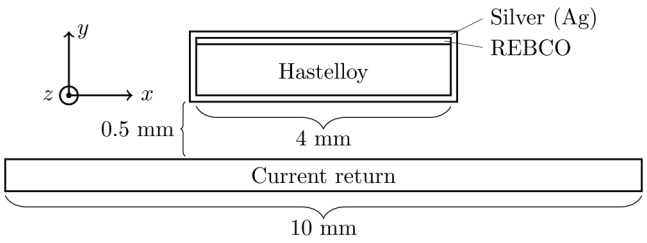

FIG. 2. Schematic of the sample geometry (not to scale). The current flows along the z direction. The tape has 1 μm of Rare-Earth Barium Copper Oxide (REBCO), 50 μm of hastelloy, and 1 μm of the surrounding silver stabilizer.

tape with a 1-μm-thick layer of REBCO deposited on a 50-μm-thick substrate of hastelloy. The entire tape is surrounded by a 1-μm-thick silver layer. A 10-mm-wide and 10-μm-thick copper conductor located 0.5 mm below the tape is also included in the simulation to model the current return path. When the latter is close to the sample and the current varies rapidly, it has an impact on the spatial current distribution (proximity effect). In addition, in the context of ultrafast current pulses, the current distribution within the sample does not become instantaneously uniform over its cross section: the self-field requires a certain time to relax and allows current to penetrate deeper in the sample. This phenomenon is called the "skin effect" in ohmic conductors, but in more general terms, it is a "magnetic relaxation" phenomenon.

The electrical and thermal properties of the nonsuperconducting materials, as well as the thermal properties of REBCO, were taken from the references given in Ref. 10. In the magnetothermal model, the electrical resistivity of REBCO was modeled with a power law characteristic, i.e.,

$$\rho = \frac{E_0}{J_c(T)}\left|\frac{J_z}{J_c(T)}\right|^{n-1}, \tag{6}$$

where J_c is the critical current density, n is the power law exponent, and E_0 is the electric field criterion used to determine I_c from V-I measurements. The temperature dependence of J_c is given by the empirical formula

$$J_c(T) = J_{c_0}\frac{(T_c - T)}{(T_c - 77\,\mathrm{K})}, \tag{7}$$

where T_c is the critical temperature and J_{c_0} is the current density at $T = 77$ K. The values of the REBCO electrical parameters used in this paper are listed in Table I. They are based on an experimental fit on data taken on a sample fabricated by SuperPower.

Note that the power law model in this paper is only used to study by simulation the dynamics of current and electric field distributions, as well as what happens when one measures voltages in the presence of fast current pulses. The final data analysis performed with the UC model does not make any assumption about the mathematical form of REBCO resistivity.

TABLE I. Parameters used for studying the electrodynamics of pulsed currents.

Param.	Value	Unit	Comment
S_{HTS}	40×10^{-6}	cm^2	HTS cross section
T_c	90	K	
E_0	1	μV/cm	
I_c	91	A	(at $T = 77$ K)
n	19	...	(at $T = 77$ K)
J_{c_0}	2.275	MA/cm^2	$J_{c_0} = \frac{I_c(77\,\mathrm{K})}{S_{HTS}}$

C. Current density and electric field profiles during pulses

The solid lines in Figs. 3(a) and 3(b), respectively, show the current density (J) and electric field (E) profiles vs time across the width of the tape defined in Fig. 2, in which we imposed a current pulse of $I_{\max} = 135$ A, $t_r = 10\,\mu$s, and $t_p = 100\,\mu$s. The initial temperature of the tape was $T_0 = 77$ K, thus $I_{\max} \approx 1.5 I_c(77\,\mathrm{K})$. It is understood that, in 2D, $J = J_z$ and $E = E_z$. We observe that, in this particular case, E and J become uniform after approximately 40 μs. At the beginning of the pulse, both J and E are much stronger at the edges of the tape than in its center. This is due to the magnetic relaxation. In superconductors, magnetic relaxation leads to a critical state profile that rapidly flattens over time when $I_{\max} \geq I_c$. The practical consequence of this relaxation is that we do not measure the same voltage if we place the voltage taps on the edge or along the center line of the tape, unless E becomes uniform across the tape width.

As a comparison, the same simulation was run on a fictitious tape with the same geometry as in Fig. 2, but where REBCO has been replaced by silver (Ag), whose resistivity is much higher than that of REBCO when the latter is in the superconducting state. The results for J and E are plotted as dashed lines in Figs. 3(a) and 3(b). We observe that J and E are much more uniform in this case.

The above results indicate that the magnetic relaxation time is longer when resistivity is low, such as in superconductors. Therefore, in order to perform meaningful voltage measurements in CCs in the presence of current pulses on the time scale of microseconds, the duration t_p of the pulses must be chosen carefully. On the one hand, one would like to make sure that the pulses are long enough so that E and J become uniform across the width of the tape before considering the measurement as valid. Otherwise, the experimental error on the resistivity could be important (it will be quantified later in this paper). On the other hand, too long pulses can lead to a thermal destruction of the sample.

D. Induced voltage and relaxation time

The simplest way to measure the relaxation time of J and E during a pulse is to use a loop placed on top of the sample, but electrically insulated from it, as shown in Fig. 4. This loop is in fact a pick-up coil in which a voltage $V_i = -\mathrm{d}\Phi/\mathrm{d}t$ is induced when the total magnetic flux linking the loop (Φ) varies with time (Faraday's equation). We can write $\Phi = \iint_{S_i} \vec{B} \cdot \mathrm{d}\vec{S}_i$, where $\vec{B}$ is the magnetic flux density and $\vec{S}_i$ is a unit vector perpendicular to the cross section S_i of the loop. As shall be seen later, Φ varies over

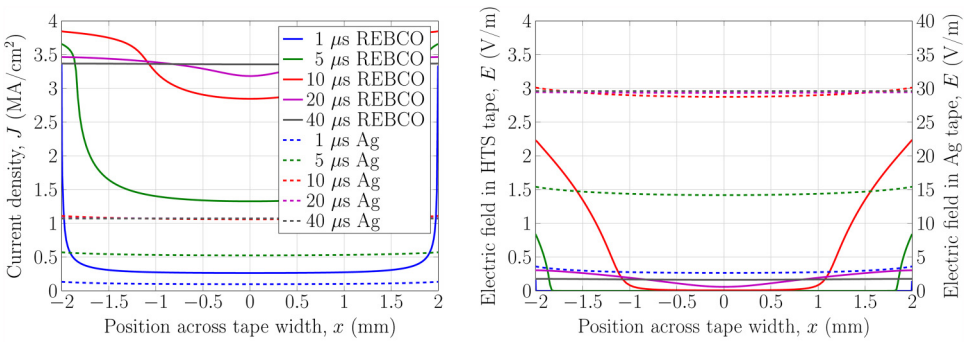

FIG. 3. Current density (a) and electric field (b) profiles simulated for a current pulse of $I_{max} \approx 1.5 I_c = 135$ A, $t_r = 10\,\mu$s, and $t_p = 100\,\mu$s in a regular REBCO CC (full lines) and in a fictitious CC, where REBCO has been replaced by silver (dashed lines). This illustrates how the presence of REBCO strongly influences the profiles and their relaxation times.

time not only when the total current $I_{tot}(t)$ in the sample changes, but also when it is constant and equal to I_{max}, but still relaxing toward a uniform distribution.

This is more easily seen by rewriting Faraday's equation in terms of the electric field. As a first step, we drop the minus sign in $V_i = -\mathrm{d}\Phi/\mathrm{d}t$, since we can always arbitrarily swap the terminals of a pick-up coil in order to change the sign of the induced voltage. We can thus write $V_i = \mathrm{d}\Phi/\mathrm{d}t = \iint_{S_i} \frac{\partial \vec{B}}{\partial t} \cdot \mathrm{d}\vec{S}_i = \iint_{S_i} \mu_0 \frac{\partial \vec{H}}{\partial t} \cdot \mathrm{d}\vec{S}_i$. In our 2D coordinate system (see Fig. 4), the integral becomes $\int_0^\ell \int_{x_1}^{x_2} \mu_0 \frac{\partial H_y}{\partial t}\, \mathrm{d}x\, \mathrm{d}z$, where ℓ is the length of the loop and $x_2 - x_1$ is its width. Finally, knowing that the normal component of $\vec{H}$ corresponds to H_y, and using (2) to write $\mu_0 \frac{\partial H_y}{\partial t} = \frac{\partial E_z}{\partial x} = \frac{\partial E}{\partial x}$, we obtain

$$\begin{aligned} V_i &= \ell \int_{x_1}^{x_2} \frac{\partial E}{\partial x}\, \mathrm{d}x, \\ &= \ell\,(E(x_2) - E(x_1)), \end{aligned} \tag{8}$$

that is, the induced voltage V_i is simply equal to the difference in the electric field values at positions x_2 and x_1, times the length ℓ of the loop. Furthermore, we clearly see that V_i is zero only if $E(x_1) = E(x_2)$, which means that the electric field E (and thus J) must be uniform across the width of the sample. The time required to reach $V_i = 0$ can, therefore, be used as a definition of the relaxation time of a current pulse.

If x_1 corresponds to the center the tape and x_2 corresponds to its edge (or side), the inductive voltage per unit length, defined as $v_i = V_i/\ell$ (V/m), can be written as

$$v_i = E^s - E^c, \tag{9}$$

where $E^c = E(x_1)$ is the electric field at the center of the tape and $E^s = E(x_2)$ is the electric field on the side of the tape.

E. Voltage measurement during pulses

The above development, leading to Eq. (8), is in fact a simplified version of the reality. It is only valid if the loop is located exactly in the same plane as that where the current flows. In practice, the loop is necessarily located slightly above the sample by at least the insulation thickness of the voltage leads.

Figure 5 shows the real geometry of the voltage measurement setup used in our experiments. The wires represented correspond to the traces of a 4-layer printed circuit board (PCB) integrated in

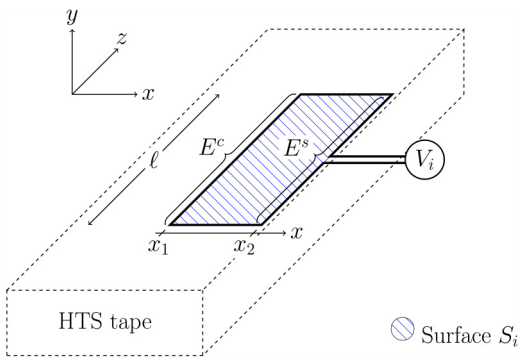

FIG. 4. Ideal geometry of an inductive loop located on the surface of a HTS tape sample. The inductive voltage is simply $V_i = -\mathrm{d}\Phi/\mathrm{d}t$, where Φ is the total flux linking the loop defined by the surface S_i.

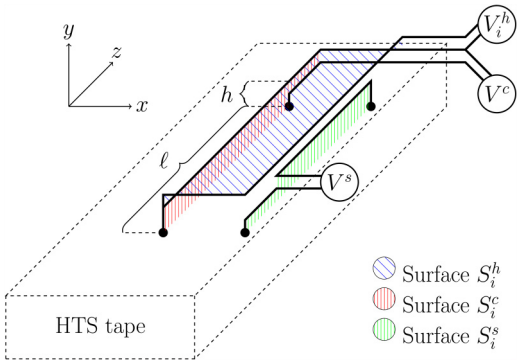

FIG. 5. Realistic geometry of a voltage measurement setup for a HTS tape, showing 4 contact points (voltage taps) on the tape surface (black dots). The different lines correspond to wires used as voltage leads for three voltmeters. For practical reasons, these wires cannot be in the sample plane as the sample surface. In our physical setup, we have $h \approx 0.7$ mm and $\ell = 3.4$ cm.

our sample holder. One sees that the traces are located at different heights above the surface of the sample. The PCB is pressed onto the surface of the sample, realizing electrical contacts at four specific points (black circles in the figure). This configuration allows measuring three quantities: (i) the total voltage V^c over a distance ℓ along the center of the tape, (ii) the total voltage V^s over a distance ℓ along the side of the tape, and (iii) the induced voltage V_i^h in a loop similar to that of Fig. 4, but whose height above the surface of the sample is $h \approx 0.7$ mm. As a result, V_i^h is slightly different from the ideal case V_i. In addition, the surface S_i^h of the loop is not contained in a well-defined plane. Finally, for practical reasons, the loop is longer than ℓ, but this is not a problem since later in this paper we normalize all measured voltages by the length of the voltage leads along z.

In practice, the useful measurements for determining the resistivity are V^c and V^s, and not V_i^h, which only allows determining the relaxation time. Since the leads of the voltmeters measuring V^c and V^s close their paths through the sample, one can write (Faraday's law in integral form)

$$\begin{aligned} V^{c,s} &= \int_{u^{c,s}} \vec{E} \cdot \mathrm{d}\vec{u}^{\,c,s} + \iint_{S_i^{c,s}} \frac{\partial \vec{B}}{\partial t} \cdot \mathrm{d}\vec{S}_i^{c,s}, \\ &= \ell E^{c,s} + V_i^{c,s}, \end{aligned} \tag{10}$$

where $\vec{E}$ and $\vec{B}$ are the local electric field and magnetic flux density, respectively; $\vec{u}^{\,c,s}$ is an integration path running from one terminal of the voltmeter to the other; $S_i^{c,s}$ is the loop surface illustrated in Fig. 5; and ℓ is the distance between the voltage taps. The term $V_i^{c,s}$, therefore, corresponds to an induced voltage due to flux from the sample linking the loop formed by the voltmeter leads, exactly as explained in Sec. II D.

To obtain the term $\ell E^{c,s}$, we assumed that the voltmeter is perfect, i.e., it draws negligible current from the sample and the electric field is zero in the voltmeter leads. Thus, the only nonzero part of the first integral in (10) is for the integration path $\vec{u}^{\,c,s}$ in the sample. At the end, the integral reduces to $\ell E^{c,s}$. We thus have

$$v^{c,s} = \frac{V^{c,s}}{\ell} = E^{c,s} + v_i^{c,s}, \tag{11}$$

where v^c and v^s are the normalized V^c and V^s voltages measured by the voltmeters at the center and on the side of the tape, respectively, and v_i^c and v_i^s are the normalized parasitic voltages associated with the same voltmeters, which prevent us from measuring directly the surface electric fields E^c and E^s. Remembering that for an ideal inductive pick-up loop, $v_i = E^s - E^c$ [see Eq. (8)], we can write

$$\begin{aligned} v_i &= E^s - E^c, \\ &= (v^s - v_i^s) - (v^c - v_i^c), \\ &= v^s - v^c + v_i^{par}, \end{aligned} \tag{12}$$

where $v_i^{par} = v_i^c - v_i^s > 0$ (a result found by simulation) is the net inductive parasitic voltage resulting from the nonideal configuration of the voltmeter leads. In practice, it means that one cannot find an equivalent to the ideal loop of Fig. 4 with two voltmeters measuring the surface electric field, because the parasitic voltage is always present. In the particular context of ultrafast current, v_i^c and v_i^s can be of the same order of magnitude than E^c and E^s, even if the surfaces S_i^c and S_i^s are small, e.g., when their thickness is less than that of a PCB. Therefore, it is necessary to wait until the end of the relaxation process before extracting any useful data. Indeed, after relaxation has completed and the current in the sample is uniform, all inductive voltages are zero, i.e., $v_i = v_i^c = v_i^s = v_{par} = 0$ and $v^s = v^c = E^s = E^c = E$, where E is the uniform static electric field measured after relaxation. Further details about these subtil voltage measurement issues can be found in Refs. 11–13.

F. Simulated voltage measurements

The magnetothermal model introduced in this section can be used to get an idea of the voltage waveforms that we should measure with the experimental setup of Fig. 5, i.e., v^c, v^s, and v_i^h, which is the closest approximation of v_i that we can obtain experimentally. To simplify the simulations, the surfaces S_i^c, S_i^s, and S_i^h shown in the figure were modeled as simple rectangular loops, i.e., their irregular paths have been neglected. The total flux variation in each loop was computed numerically in order to obtain the inductive voltages v_i^c, v_i^s, and v_i^h.

Figure 6 shows an example of results obtained for v_i^h, E^c, E^s, $v^c = E^c + v_i^c$, and $v^s = E^s + v_i^s$, for a current pulse with $I_{\max} = 150$ A $[\approx 1.65 I_c(77\,\mathrm{K})]$ and $t_r = 10\,\mu$s. We can clearly see that E^c remains at zero for a much longer time than E^s, since it takes time for the current to relax and reach the center of the sample. Also, the time evolution of E^s and E^c in the current plateau purely results from the relaxation (there are no parasitic voltages here since the simulation allows obtaining directly the electric field values). The effect of induced voltages can be seen on the v^c and v^s curves though the difference between the $v^{c,s}$ and $E^{c,s}$ curves corresponds to the parasitic induced voltages $v_i^{c,s}$. Although during the relaxation stage $v_i^s\,(= v^s - E^s)$ is quite negligible in this particular case, $v_i^c\,(= v^c - E^c)$ is not negligible at all. Interestingly, for $t \geq 15 - 20\,\mu$s, v^c reaches a constant value that approaches the

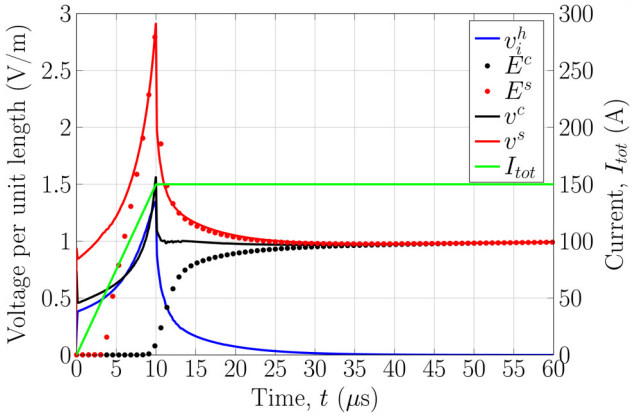

FIG. 6. Simulated values of v_i^h, E^c, E^s, v^c, and v^s for a current pulse of $I_{\max} = 150$ A $[\approx 1.65 I_c(77\,\mathrm{K})]$ and $t_r = 10\,\mu$s. The sample temperature was also simulated, but results are not shown here.

asymptotical value of E^c and E^s, despite the fact that the relaxation is not yet complete. This is a coincidence though, since the exact shape of v_i^c highly depends on the geometries of the sample and sample holder. In order to conclude that E^c and E^s have both relaxed to their final value, as in Fig. 6, one needs at least one additional measurement, either v^s or v_i^h.

G. Experimental validation of voltage measurement simulations

In order to validate the simulated voltage measurements obtained with our electromagnetic model, i.e., Eqs. (1)–(3), we measured the electrical response of a 4-mm-wide and 50.8-μ(m-thick copper strip immersed in liquid nitrogen and submitted to a 15 kHz, 16.9 A peak-to-peak AC current. The use of a high frequency and of liquid nitrogen allowed us in decreasing the skin depth $\delta = \sqrt{2\rho/(\omega\mu_0)}$ in copper to $\approx$0.2 mm [$\rho_{Cu}(77\,\mathrm{K}) \approx 0.25\,\mu\Omega\,\mathrm{cm}$]. A small skin depth allows increasing the difference between v^c and v^s sufficiently to make it measurable. A lock-in amplifier was used to measure v^c, v^s, and v_i^h, which have also been simulated with our model. The geometry of the leads used to measure the voltages is illustrated in Fig. 5.

The results are compared in Fig. 7. We observe that the experimental values and the simulations are in excellent agreement, which validate our electromagnetic model. The very small discrepancy observed for v_i^h comes from the irregularities in the experimental inductive loop, which was simulated as a planar rectangle in COMSOL.

III. MODEL FOR DATA ANALYSIS

A. Uniform current (UC) model

The magnetothermal (MT) model used in the Sec. II is accurate, but it has two drawbacks. Firstly, it requires an *a priori* knowledge of the functional form of the resistivity $\rho(J, T)$, which we do not have since we are trying to measure it with this pulsed current experiment. Therefore, the MT model cannot be used directly as a postprocessing tool. Secondly, even if it could be used, it would require substantial computational resources, typically more than 5 min per simulated pulse, which is too much for being practical for postprocessing data. In practice, the only available experimental data are (i) the total current $I_{tot}(t)$ injected in the sample, (ii) normalized voltage measurements [at least $v^c(t)$, and ideally also $v^s(t)$ and/or v_i^h], and (iii) the initial temperature T_0 of the sample (there is no possibility to measure the temperature evolution in real time during a pulse). Our postprocessing tool must be able to work with this sole information.

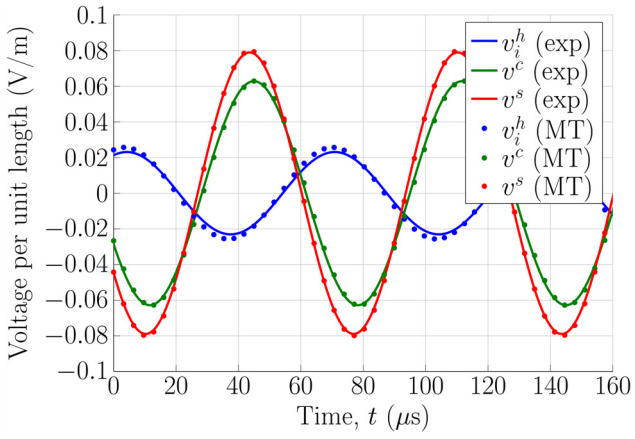

FIG. 7. Comparison between the experimental voltages (exp) and the voltages simulated with the magnetothermal (MT) model, when a 15 kHz AC current of 16.9 A peak-to-peak AC is imposed in a 4-mm-wide and 50.8-μm-thick copper strip immersed in liquid nitrogen. The voltage leads configuration is illustrated in Fig. 5.

We, therefore, propose to replace the full electromagnetic model by a simple 2D static current sharing model, in which E is uniform over the whole cross section of the tape at all times and J is uniform over the cross section of the superconducting layer. The 2D time transient thermal model remains the same as above. We shall call this model the Uniform Current (UC) model.

In the UC model, we assume that the static electric field E^{UC} supporting the current flow is equal to the voltage per unit length measured at the center of the tape, i.e., $E^{UC} = v^c$. The local current density in silver and hastelloy can be easily calculated with

$$J_{Ag}^{UC} = \frac{v^c}{\rho_{Ag}(T)}, \tag{13}$$

$$J_{Hast}^{UC} = \frac{v^c}{\rho_{Hast}(T)}, \tag{14}$$

where ρ is the local resistivity of the material, which is known for silver and hastelloy, and T is the local temperature. The total currents flowing into silver and hastelloy are given by $I_{mat}^{UC} = \int_{S_{mat}} J_{mat}^{UC}\,\mathrm{d}x\,\mathrm{d}y$, where $mat = \{Ag, Hast\}$ and S_{mat} is the cross section of the material. These integrals are easily computed numerically. The current I_{HTS}^{UC} flowing in the superconductor is obtained by subtracting the current of each metallic layer from the total measured current (I_{tot}), i.e.,

$$I_{HTS}^{UC} = I_{tot} - I_{Ag}^{UC} - I_{Hast}^{UC}. \tag{15}$$

The current density J_{HTS}^{UC} in the superconductor, assumed as uniform by definition of the UC model, is given by

$$J_{HTS}^{UC} = \frac{I_{HTS}^{UC}}{S_{HTS}}, \tag{16}$$

where S_{HTS} is the cross section of the superconductor. Finally, the resistivity ρ_{HTS}^{UC} of the superconductor is expressed as

$$\rho_{HTS}^{UC} = \frac{v^c}{J_{HTS}^{UC}}, \tag{17}$$

which is the most important result of this development.

Once the current density is known in all materials, we calculate the local losses $Q = E^{UC} J_{mat}^{UC} = v^c J_{mat}^{UC}$ and we insert these

values in heat Eq. (5) to compute the temperature distribution over the whole tape cross section.

The UC model is easy to use. Although it is convenient to solve it with the finite element method, other numerical or analytical methods could be used. In all cases, the UC model induces two sources of error in the solution. Firstly, because the model computes an instantaneous current sharing between the various tape materials, it neglects all relaxation effects, which has an impact on the value of local losses and temperature. Secondly, we know that v^c is not equal to the electric field in the sample during the relaxation stage, since it includes an additional induced voltage term, i.e., $v^c = E^c + v_i^c$, with $v_i^c > 0$, thus $v^c > E^c$. Based on the physical layout of our voltage measurement setup (see Fig. 5), and assuming that $I_{tot} = I_{\max}$ is constant, as it is during the pulse plateau, we can bound on the relative error $\xi^{UC}_{\rho_{HTS}}$ on the resistivity calculated with the UC model, ρ^{UC}_{HTS}, i.e.,

$$\xi^{UC}_{\rho_{HTS}} = \left|\frac{\langle\rho\rangle_{HTS} - \rho^{UC}_{HTS}}{\rho^{UC}_{HTS}}\right| \leq \left|\frac{v_i^h}{v^c}\right|, \tag{18}$$

where $\langle\rho\rangle_{HTS}$ is the real average resistivity of the superconductor, defined as $\langle\rho\rangle_{HTS} = \frac{1}{S_{HTS}}\iint_{S_{HTS}} \rho_{HTS}(x,y)\,dx\,dy$, but unknown when performing the experiment. The proof of this expression is developed in the Appendix. To obtain (18), we assume that the values of E and J are minimal in the center and maximal on the side of the sample, but no other assumption is made about the form of the resistivity. From a practical point of view, one just need to remember that $\max\left(\xi^{UC}_{\rho_{HTS}}\right) = \left|v_i^h/v^c\right|$.

Equation (18) explicitly shows that the error $\xi^{UC}_{\rho_{HTS}} \to 0$ only when $v_i^h \to 0$, i.e., when relaxation disappears and E and J get uniform in the superconductor (here we neglect the slight dependence of J_c with the local self-field). However, even if we reach a steady state regime in the pulse plateau, where the UC model is highly accurate, the transient electromagnetic regime that precedes this steady state may induce an offset error in the temperature and current sharing calculated with the UC model. This error is quantified in Sec. III B.

B. Accuracy of UC model

In this section, we use reference solutions generated with the magnetothermal solver in order to evaluate the error committed by the UC model in recomputing the temperature and current sharing. The geometric parameters used in the simulations are those illustrated in Figs. 2 and 5. The superconductor behavior is still based on a power law model whose parameters are given in Table I. Current pulses with $t_r = 10\,\mu$s, $t_p = 100\,\mu$s, and various $I_{\max}$ were simulated (see Fig. 1 for pulse waveform definition).

The following procedure was used in order to emulate a perfect experiment. Firstly, the magnetothermal model was used to solve each problem and to determine the parasitic inductive voltage $v_i^c(t)$ and the electric field $E^c(t)$ along the center of the tape. From these values, we deduced $v^c(t) = E^c(t) + v_i^c(t)$, which is the simulated value of the voltmeter reading (perfect reading, without noise or other experimental error). Next, this $v^c(t)$ value was used as an input to the UC model, as well as the total current $I_{tot}(t)$ and the initial sample temperature ($T_0 = 77\,$K in all cases). Then, we

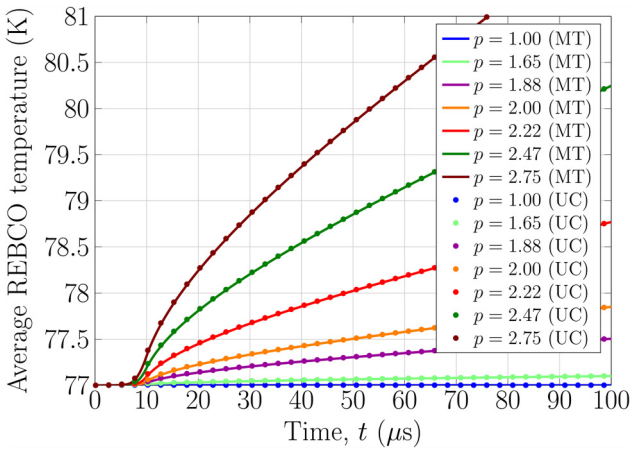

FIG. 8. Average temperature of the superconductor obtained with the magnetothermal (MT) model and the uniform current (UC) model for current pulses with $t_r = 10\,\mu$s, $t_p = 100\,\mu$s, and different $p = I_{\max}/I_c(77\,\text{K})$.

quantify the relative errors committed on $\langle T\rangle^{UC}_{HTS}$, I^{UC}_{HTS}, and ρ^{UC}_{HTS} with respect to the reference values from the magnetothermal model, i.e., $\langle T\rangle^{MT}_{HTS}$, I^{MT}_{HTS}, and $\langle\rho\rangle^{MT}_{HTS}$ (averaging is performed on the HTS cross section).

Figure 8 compares the average REBCO temperatures obtained with the magnetothermal model, $\langle T\rangle^{MT}_{HTS}$, with those obtained with the UC model, $\langle T\rangle^{UC}_{HTS}$, for different values of $p = I_{\max}/I_c(77\,\text{K})$. We observe that they are almost the same, even if the maximum temperature elevation is above 4 K in the worst case ($p = 2.75$). The maximum relative error recorded was less than 0.025%, which is very satisfying considering that it is much lower than any experimental source of error.

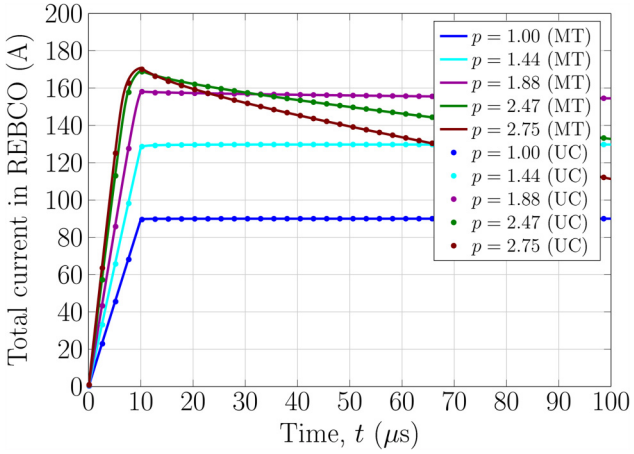

FIG. 9. Total current in the superconductor obtained with the magnetothermal (MT) model and the uniform current (UC) model for current pulses with $t_r = 10\,\mu$s, $t_p = 100\,\mu$s, and different $p = I_{\max}/I_c(77\,\text{K})$.

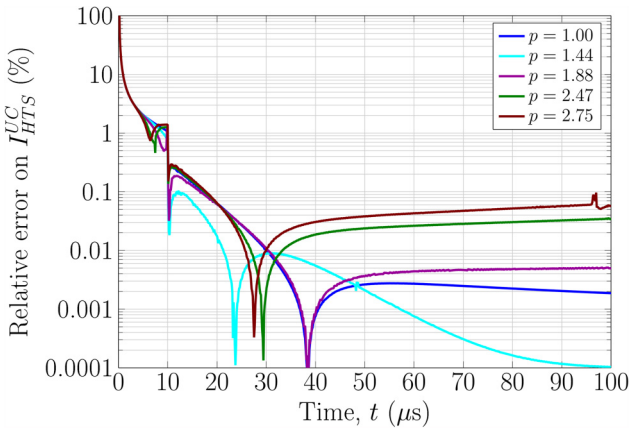

FIG. 10. Absolute value of relative error on current in REBCO calculated with the UC model, for the same values of p as in Fig. 9.

Figure 9 compares the currents in the superconductor obtained with the magnetothermal model, I_{HTS}^{MT}, with those obtained with the UC model, I_{HTS}^{UC}. The relative errors are shown in Fig. 10. We observe that I_{HTS}^{UC} is very accurate (less than 1% of error) as soon as the total current in the sample is constant, i.e., for $t > 10\,\mu$s in this case. The large error (between 1% and 100%) observed during the current rise is a consequence of the parasitic induced voltage v_i^c, which artificially increases the value of $v^c\,(= E^c + v_i^c)$ and, according to (13) and (14), this leads to an exaggeration of the currents flowing into silver (I_{Ag}^{UC}) and hastelloy (I_{Hast}^{UC}), and thus an underestimation of I_{HTS}^{UC}, as can be deduced from (15). Note that the decrease of I_{HTS} over time for $p = I_{\max}/I_c(77\,\mathrm{K}) \geq 1.88$ is caused by heating of the REBCO layer, which increases the superconductor resistance and forces more current to flow in the other metallic layers (silver and hastelloy).

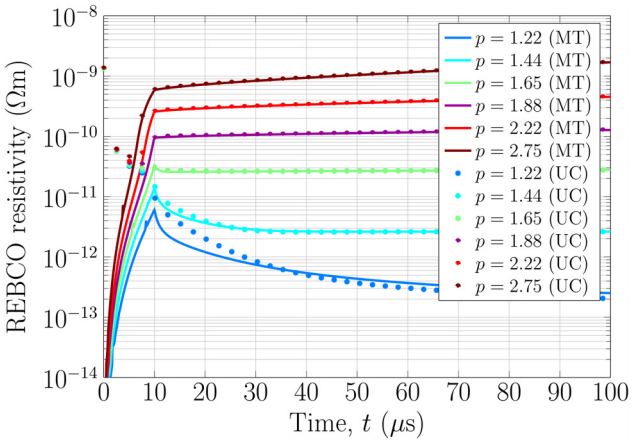

FIG. 11. REBCO resistivity obtained with the magnetothermal (MT) model and the uniform current (UC) model, for current pulses with $t_r = 10\,\mu$s, $t_p = 100\,\mu$s, and different $p = I_{\max}/I_c(77\,\mathrm{K})$.

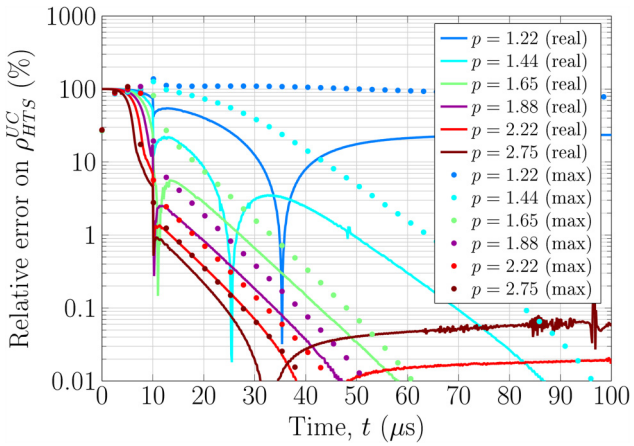

FIG. 12. Solid lines: absolute value of $\xi_{\rho_{HTS}}^{UC}$ (real), for the same values of p as in Fig. 11. Symbols: upper bound of the relative error (max), calculated with (18).

Figure 11 compares the REBCO resistivities obtained with the magnetothermal and the UC models, respectively, $\langle\rho\rangle_{HTS}^{MT}$ and ρ_{HTS}^{UC}. As expected, the UC model gives a completely wrong value of resistivities during the current rise ($t < 10\,\mu$s). Once again, this error is mainly a consequence of the parasitic voltage v_i^c. However, as soon as the applied current becomes constant (for $t > 10\,\mu$s), the two models are in better agreement, especially for current pulses with $I_{\max} > 1.5 I_c(77\,\mathrm{K})$, since in this case the current relaxes rapidly in the sample.

The error is better quantified by looking at Fig. 12, which shows the relative error induced by the UC model, together with the upper bound error defined in (18), i.e., $\max\left(\xi_{\rho_{HTS}}^{UC}\right) = \left|v_i^h/v^c\right|$, evaluated with the reference solutions from the magnetothermal model. The results strongly support the fact that the upper bound proposed is very conservative and that it provides a worst-case scenario to determine the minimum pulse duration required for the relaxation to die out before thrusting the measured value of ρ_{HTS}^{UC}. We note that for very low values of $p = I_{\max}/I_c(77\,\mathrm{K})$, say, $p < 1.25$, the UC model never gets close to the correct resistivity value (relaxation time too long, at least much longer than the pulse duration). In this case, one could use longer pulses in order to obtain measurements with an acceptable level of error $\xi_{\rho_{HTS}}^{UC}$.

IV. EXPERIMENTAL RESULTS

A. Measurements on 2G HTS CCs in over-critical current conditions

The sample used for our experimental validation was a commercial 2G HTS CC obtained from SuperPower. Its geometry is depicted in Fig. 2. At $T_0 = 77\,\mathrm{K}$ and in self-field conditions, we measured a critical current $I_c(77\,\mathrm{K}) = 91\,\mathrm{A}$ (electric field criterion $E_0 = 1\,\mu\mathrm{V/cm}$) and a n-value of 19 (fit of a power law model on the experimental V-I curve). These values were used in the simulations presented earlier (see Table I).

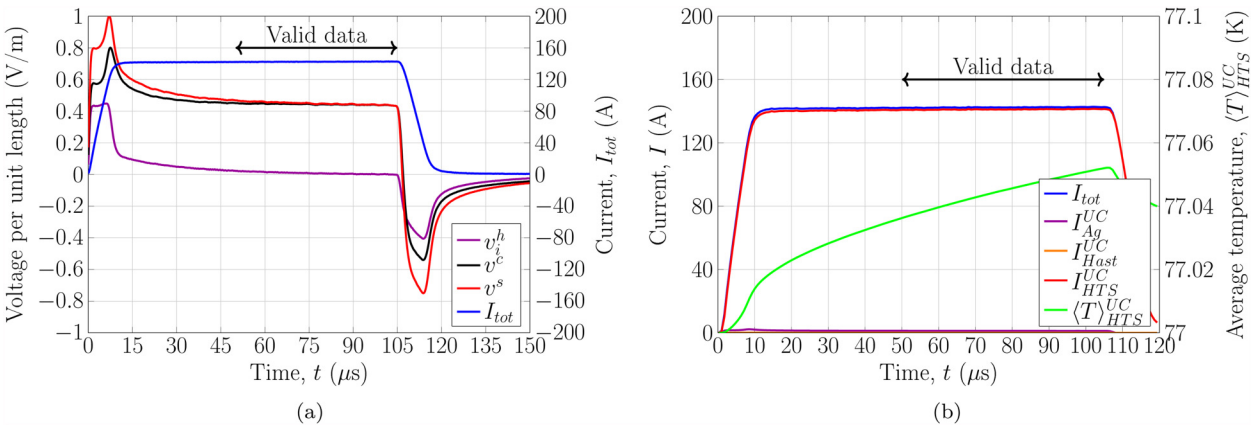

FIG. 13. (a) Current and voltages measured for a pulse of $t_r = 10\,\mu$s and $I_{max} = 144$ A [$\approx 1.6 I_c(77\,\text{K})$]; (b) currents in each layer of the tape and average HTS layer temperature $\langle T\rangle_{HTS}^{UC}$, calculated *a posteriori* with the UC model. Valid data range was determined using the condition $|v_i^h/v^c| < 5\%$.

Current pulses with $t_r = 10\,\mu$s and I_{max} varying between 109 A and 251 A were injected in the sample. For all measurements, the sample was immersed in a 77 K liquid nitrogen bath, which fixed the initial sample temperature T_0 to 77 K. Selected measurements are presented in Figs. 13–15, corresponding to low, medium, and high over-current conditions, respectively. In each case, the measured current and voltages are shown in part (a) of the figure, and the current sharing and average HTS temperature calculated with the UC model are shown in part (b).

Figure 13(a) presents the voltages measured in the case of a 144 A pulse [$\approx 1.6 I_c(77\,\text{K})$], considered a low over-current condition. At this current level, the temperature rise can be neglected (less than 50 mK), as can be seen in Fig. 13(b). For this case, the shape of the voltage is mostly influenced by magnetic relaxation effects. The experimental results in Fig. 13(a) are qualitatively similar to those of Fig. 6 (finite element simulations): the peak in $v^s(t)$ is larger than the peak in $v^c(t)$, and $v_i^h \to 0$ as $(v^s - v^c) \to 0$, proving that v_i^h is a reliable indicator of the magnetic relaxation rate. The differences between the experimental results and the simulations come mostly from: (i) the nonideal ramping rate in the experiment (not perfectly constant at the beginning and end of the ramp), (ii) the different levels of current applied in the experiment (144 A) and in the simulation (150 A), and (iii) the unverified physical representativeness of the empirical resistivity model used to generate Fig. 6. In this particular case, one could say that all data points in the interval $50\,\mu\text{s} \le t \le 105\,\mu\text{s}$, corresponding to $|v_i^h/v^c| < 5\%$, could be considered reliable to populate the surface $\rho_{HTS}^{UC}(J(t), T(t)) = v^c(t)/J_{HTS}^{UC}(t)$, where $J_{HTS}^{UC} = I_{HTS}^{UC}/S_{HTS}$ and $T(t)$ are taken from Fig. 13(b). This is illustrated at the end of this section.

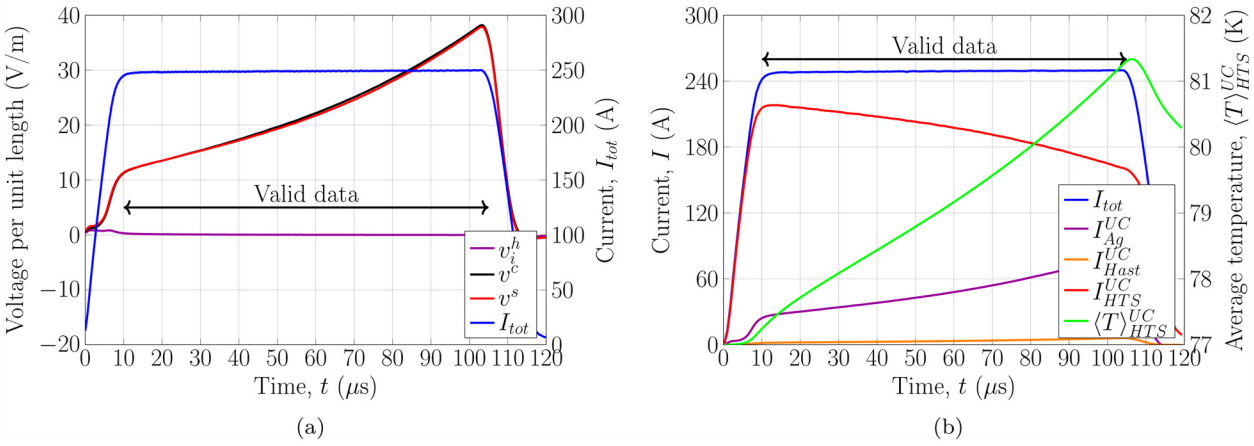

FIG. 14. (a) Current and voltages measured for a pulse of $t_r = 10\,\mu$s and $I_{max} = 251$ A [$\approx 2.75 I_c(77\,\text{K})$]; (b) currents in each layer of the tape and average HTS layer temperature $\langle T\rangle_{HTS}^{UC}$, calculated *a posteriori* with the UC model. Valid data range was determined using the condition $|v_i^h/v^c| < 5\%$.

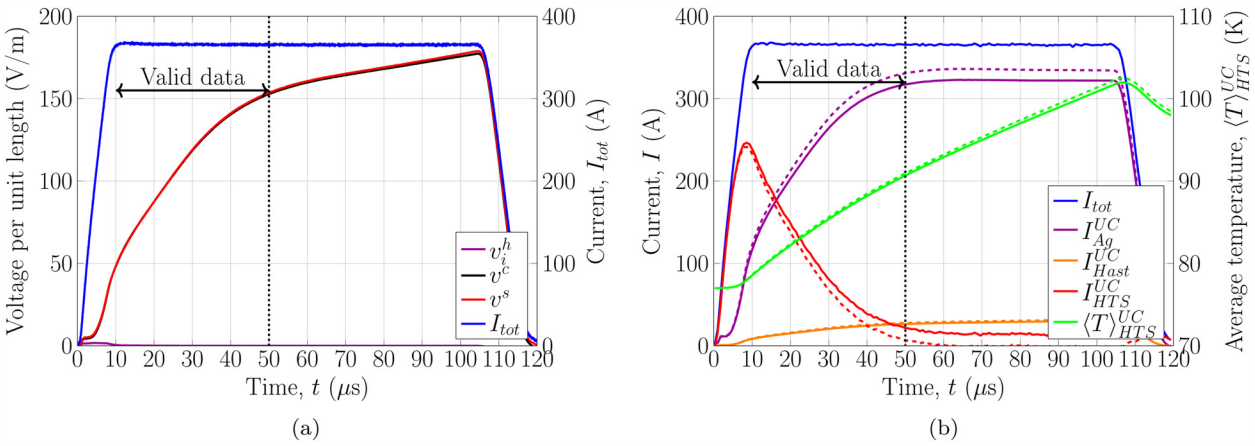

FIG. 15. (a) Current and voltages measured for a pulse of $t_r = 10\,\mu$s and $I_{max} = 367$ A [$\approx 4I_c(77\,\text{K})$]; (b) currents in each layer of the tape and average HTS layer temperature $\langle T \rangle_{HTS}^{UC}$, calculated *a posteriori* with the UC model. The dotted black line at $t = 50\,\mu$s corresponds approximately to $\langle T \rangle_{HTS}^{UC} = T_c$. The dashed lines correspond to the UC model results obtained after increasing $v^c(t)$ by 5%. Valid data range was determined using $|v_i^h/v^c| < 2\%$.

Figure 14(a) presents the voltages measured in the case of a 251 A pulse [$\approx 2.75I_c(77\,\text{K})$], considered a medium over-current condition. In this case, the temperature rise cannot be neglected. One can see in Fig. 14(b) that $\langle T \rangle_{HTS}^{UC}$ increases by more than 4 K during the pulse. Note that the decrease in temperature at the end of the pulse is caused by heat diffusion toward the substrate, and not to any form of cooling of the tape, since the UC model considers adiabatic conditions. Going back to the measured voltages, we observe a parabolic curvature in the v^c and v^s voltages, which is correlated with the temperature rise. However, the difference between v^c and v^s in this case is very small (below the accuracy of the voltage measurements) as compared to the common mode (resistive) signal, which indicates that the magnetic relaxation time is negligible for the whole pulse duration (below 5%). Therefore, in this case, one can use all data points in the interval $10\,\mu\text{s} \leq t \leq 103\,\mu$s to populate the $\rho_{HTS}^{UC}(J(t), T(t))$ surface. One can still assess if there is any small magnetic relaxation effect in the sample by looking at v_i^h, which can be measured on a small scale voltage scale if needed. Finally, it is interesting to observe in Fig. 14(b) the current sharing between the HTS and silver layers. As the $\langle T \rangle_{HTS}^{UC}$ increases, ρ_{HTS}^{UC} also increases, so more and more current goes into the parallel silver layer, which has a lesser temperature dependence. A small fraction of current also flows into the hastelloy substrate.

Figure 15(a) presents the voltages measured in the case of a 367 A pulse [$\approx 4I_c(77\,\text{K})$], considered as a high over-current condition. The same comments as in Figure 14 apply to v^c, v^s, and v_i^h, except that we observe an abrupt change of slope near $t = 50\,\mu$s. This can be explained by looking at the temperature rise in Fig. 15(b): we see that $\langle T \rangle_{HTS}^{UC}$ reaches T_c 9≈90 K) near $t = 50\,\mu$s. Therefore, the change of slope indicates the moment at which the REBCO layer quenches. After the quench, the current in the HTS layer should be nearly zero, but instead we observe a small residual current of ≈10 A for $t > 50\,\mu$s. This is not physical and can result from (i) an experimental error on the voltage measurement and/or (ii) a bad knowledge of the silver resistance per unit length in the UC model, which is very likely since it is hard to know exactly the silver cross section in a tape segment (silver is never completely uniform along the tape length). Note that the latter error has an impact on the heat capacity of the tape and on the heat generation in the UC model, which can in turn impact the calculated temperature rise and the resulting current sharing, etc. For instance, if we scale the measured $v^c(t)$ curve by a factor of 1.05 (5% relative increase), we find the dashed lines shown in Fig. 15(b). With this arbitrary correction, $I_{HTS}^{UC} \to 0$ after the quench, which is more physical and confirms that the results are quite sensitive to only a few percent of accuracy on any problem input. Hence, for this pulse, we could accept the data points in the interval $10\,\mu\text{s} \leq t \leq 50\,\mu$s because, for these time values, the error caused by the UC model approximation is below 2%.

In Fig. 16, all valid data points for ρ_{HTS}^{UC} taken on the time intervals identified in Figs. 13–15 were plotted on a common graph in the (J, T) plane. The amount of data on this graph is not sufficient to define the complete $\rho_{HTS}^{UC}(J, T)$ surface of this REBCO superconductor sample, but it indicates clearly how we could eventually populate the entire surface if we managed to perform enough measurements at different initial temperatures and current amplitudes. Interestingly (and quite surprisingly), increasing the pulse duration at high current is a good approach to populate rapidly a large portion of the (J, T) plane with a single pulse, thanks to the increase in temperature during the pulse (group of points 2 and 3 in Fig. 16). Without heating, a single pulse provides only a single point in the plane (point 1 in Fig. 16). Complete characterizations of HTS samples and sensitivity analyses will be the object of further work. An example of such a characterization using the UC model can be found in Ref. 14.

B. Relaxation time

As discussed earlier, the UC model provides valid postprocessed resitivity data only after relaxation has completed. In Fig. 12,

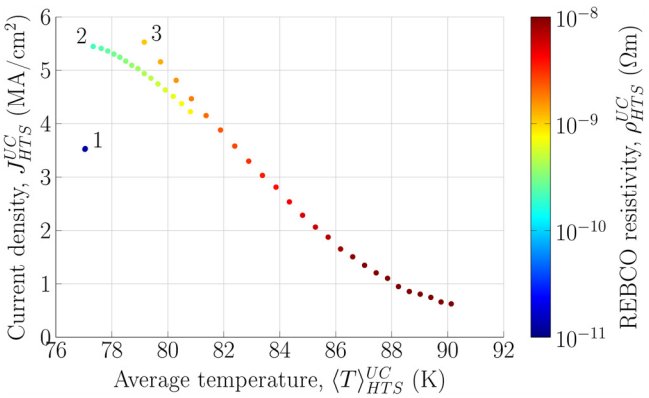

FIG. 16. REBCO resistivity vs J and T, obtained from the three cases presented in Sec. IV A. More specifically, data points identified as 1, 2, and 3 were determined from the curves presented in Figs. 13, 14, and 15, respectively (only the intervals identified as valid were used).

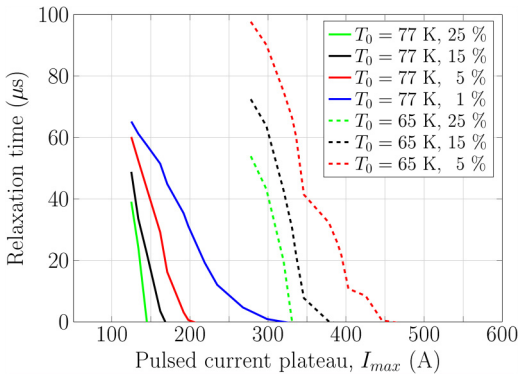

FIG. 18. Minimum pulse plateau duration t_p^{min} vs plateau current I_{max} required to keep the measured resistivity ρ_{HTS}^{UC} below a maximum error threshold. Data taken at two different initial temperatures are shown, i.e., $T_0 = 77$ K and $T_0 = 65$ K. Data for $T_0 = 77$ K were taken directly from Fig. 17.

we plotted in dotted lines the upper bound of the error due to relaxation, defined in (18) as $\max\left(\xi_{\rho_{HTS}}^{UC}\right) = |v_i^h/v^c|$, using numerical simulations. We now do the same exercise with experimental values of v_i^h and v^c, obtained from a series of pulsed current measurements realized on the same sample as in Sec. IV A. All pulses began at $t = 0\,\mu$s and reached their maximum current at $t = 10\,\mu$s, and they all had an initial temperature of $T_0 = 77$ K.

The results are shown in Fig. 17. Similarly as with the simulated results, the maximum error on ρ_{HTS}^{UC} decreases as the current pulses get higher. The experimental values are not the same as the simulated ones though, since the real resistivity is likely to differ from the empirical resistivity model used for the simulations. As we get close to I_c ($p \to 1$), the maximum relative error caused by relaxation remains relatively high (more than 20%) and decreases very slowly over time. It is difficult to establish a rule though the error will vary a lot depending on the specific sample being measured. The physical layout of the sample holder will also have an impact on the error values. Finally, uncertainty and noise on the measured voltages can also slightly bias the estimated error bound.

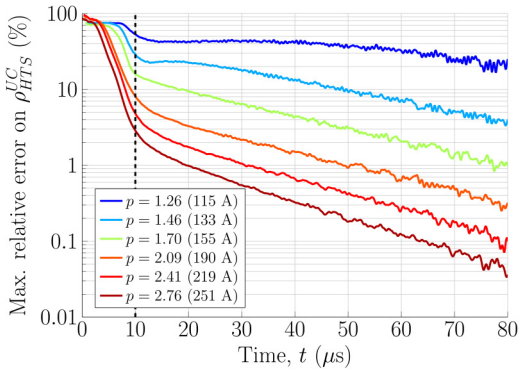

FIG. 17. Maximum relative error on HTS measured resistivity ρ_{HTS}^{UC}, for a REBCO tape with $T_0 = 77$ K, for various pulses with $p = I_{max}/I_c(77\,\text{K})$. All pulses began at $t = 0\,\mu$s and reached their maximum constant current at $t = 10\,\mu$s (dashed black line). The error plotted could be biased by noise and uncertainty on voltage measurements.

From an experimental point of view, it is useful to determine the minimum pulse duration that produces a resistivity measurement below a given error threshold (once again, this error includes only the contribution of magnetic relaxation). This can easily be done from the data of Fig. 17, and the results are plotted in Fig. 18. A similar exercise was also done on a set of data taken on the same sample, but with $T_0 = 65$ K as initial temperature, leading to higher currents since $I_c(65\,\text{K}) > I_c(77\,\text{K})$. In both cases, the rise time $t_r = 10\,\mu$s was not counted in the pulse duration, as the UC model is not accurate in this region. Only the time t_p of the pulse plateau was counted. In practice, Fig. 18 can be built with a reduced set of measurements, which can then be used to properly plan a more complete set of pulsed current measurements.

V. CONCLUSION

In this paper, we showed that the pulsed current measurement technique can be applied to characterize the resistivity of the RECBO layer in coated conductors over a wide range of current density and electric field values, provided that we pay attention to two major points: (i) magnetic relaxation and (ii) heating effects. At low currents, i.e., near I_c or slightly above, heating is negligible, but the magnetic relaxation time can be long (from milliseconds to seconds). It is thus important to use a pulse duration that is longer than the relaxation time, which can be characterized from a few preliminary measurements. These measurements should ideally involve an inductive pick-up loop, in addition to the conventional pair of voltage taps. At high currents (much above I_c), the magnetic relaxation time is very fast (scale of microseconds), but the sample temperature rises rapidly and cannot be neglected. In this case, the current sharing between the various conducting layers of the

coated conductor must be taken into account in order to extract correct $\rho(J, T)$ resistivity values.

In order to allow coherent postprocessing of all the current and voltage measurements obtained with the pulsed current measurement technique, we proposed the Uniform Current model (UC model), which consists in a simple static current sharing model coupled with a 2D thermal solver. This model takes in input the coated conductor geometry, the material properties (except that of REBCO, which is unknown), as well as the experimental voltage and current curves, and it returns in output the calculated average resistivity of the superconductor vs the average current density and temperature over its cross section, noted $\rho^{UC}_{HTS}(J^{UC}_{HTS}, \langle T\rangle^{UC}_{HTS})$. This is the closest approximation of the local resistivity one can get with such macroscopic V-I measurements. Note that the resistivity extracted with pulsed current measurements and the UC model does not assume any predefined E-J relationship: it returns only triplets of points, i.e., ρ^{UC}_{HTS}, J^{UC}_{HTS}, and $\langle T\rangle^{UC}_{HTS}$. It is up to the user to find a mathematical relationship that reproduced these data if required.

We also derived an upper bound value for the relative error associated with magnetic relaxation on the measured resistivity. This error bound is simply written as $\max\left(\xi^{UC}_{\rho_{HTS}}\right) = |v^h_i/v^c|$, where v^h_i is the voltage induced in a loop located just above the sample surface and v^c is the conventional resistive voltage drop along the center of the sample (see Fig. 5). Finite element simulations with a full magnetothermal model were used to show that this error bound is very conservative, but since it is easy to apply experimentally, it seems a good guideline to follow.

Although this paper did not address in detail the impact of various coated conductor architectures or pulsed current rising rates, all the conclusions remain valid. However, the impact of an externally applied field on the error bound proposed and on the UC model accuracy should be investigated in future work. Another way of improvement would be to try reducing the 2D thermal solver to a simpler 1D version across the thickness of the tape. This would speed up considerably the data processing.

ACKNOWLEDGMENTS

The authors gratefully thank Mr. Nicolò Riva and Dr. Bertrand Dutoit for fruitful discussions and for providing access to EPFL facilities for performing the measurements at 65 K presented in this paper. This work was funded by the Natural Sciences and Engineering Research Council of Canada (NSERC).

APPENDIX: ERROR BOUNDS ON RESISTIVITY

Assuming self-field conditions, constant current, and homogeneous resistivity in the REBCO layer, the electric field E and the current density J have their minimum value in the center of the tape and their maximum value on its edges. These conditions can be written as

$$E^s \geq E(x) \geq E^c, \tag{A1}$$

$$J^s \geq J(x) \geq J^c. \tag{A2}$$

Since the resistivity $\rho(J) = E(J)/J$ of a superconductor increases with J, we have $\rho(x_s) \geq \rho(x) \geq \rho(x_c)$, which we can also write

$$\frac{E^s}{J^s} \geq \rho(x) \geq \frac{E^c}{J^c}. \tag{A3}$$

From numerical simulations, and based on the experimental arrangement illustrated in Fig. 5, in which $S^h_i \gg S^c_i$, we could verify that, once the current is constant, $v^h_i > v^c_i$ and that $v^s_i \ll E^s$. This allows us to write

$$v^c - v^h_i = E^c + v^c_i - v^h_i \leq E^c, \tag{A4}$$

$$v^s = E^s + v^s_i \approx E^s. \tag{A5}$$

Inserting (A4) and (A5) into (A1), we obtain

$$v^s \geq E(x) \geq v^c - v^h_i, \tag{A6}$$

which can be in turn inserted into (A3) to obtain

$$\frac{v^s}{J^s} \geq \rho(x) \geq \frac{v^c - v^h_i}{J^c}. \tag{A7}$$

Now, let us define $\langle J(x)\rangle$ as the average current density in the REBCO cross section. From (A2), we can easily deduce that $\langle J(x)\rangle \leq J^s$ and $\langle J(x)\rangle \geq J^c$. We can use this fact to replace J^s and J^c by $\langle J(x)\rangle$ in (A7), which leads to

$$\frac{v^s}{\langle J(x)\rangle} \geq \rho(x) \geq \frac{v^c - v^h_i}{\langle J(x)\rangle}. \tag{A8}$$

Subtracting $v^c/\langle J(x)\rangle$ in each member of (A8) and dividing by $v^c/\langle J(x)\rangle$, we obtain

$$\frac{v^s - v^c}{v^c} \geq \frac{\rho(x) - \frac{v^c}{\langle J(x)\rangle}}{\frac{v^c}{\langle J(x)\rangle}} \geq \frac{-v^h_i}{v^c}. \tag{A9}$$

We know from (12) that $v_i \geq v^s - v^c$. Harder to show is that we also have $v^h_i \geq v^s - v^c$. The mathematical proof requires to solve for the vector potential along the entire 3D path of the loop, but one can easily see by simulation that it is always true. It was also verified experimentally. In addition, since the UC model provides a unique value J^{UC}_{HTS} for the current density in the REBCO layer, it makes sense to say that it is equivalent to the average current density $\langle J(x)\rangle$ defined above, so we assume that $J^{UC}_{HTS} = \langle J(x)\rangle$. We can thus rewrite (A9) as

$$\frac{v^h_i}{v^c} \geq \frac{\rho(x) - \frac{v^c}{J^{UC}_{HTS}}}{\frac{v^c}{J^{UC}_{HTS}}} \geq \frac{-v^h_i}{v^c}. \tag{A10}$$

Remembering that $\rho^{UC}_{HTS} = \frac{v^c}{J^{UC}_{HTS}}$ and acknowledging that the inequality remains valid if $\rho(x)$ is replaced by its average $\langle\rho(x)\rangle_{HTS}$, taken

over the cross section of the REBCO layer, we can rewrite (A10) as

$$\frac{v_i^h}{v^c} \geq \frac{\langle \rho(x) \rangle_{HTS} - \rho_{HTS}^{UC}}{\rho_{HTS}^{UC}} \geq \frac{-v_i^h}{v^c}. \tag{A11}$$

We recognize the middle term as a relative error on ρ_{HTS}^{UC}, which we denote as $\xi_{\rho_{HTS}}^{UC}$. We can thus rewrite (A11) in it final form as

$$\xi_{\rho_{HTS}}^{UC} \leq \left| \frac{v_i^h}{v^c} \right|. \tag{A12}$$

This completes the proof of Eq. (18) of this paper.

REFERENCES

[1]J. M. Doval, J. Maza, C. Torron, J. A. Veira, M. Tello, and F. Vidal, "New measurements of the transition to the normal state induced by high current densities in high-Tc superconductor microbridges under thermal smallness conditions," Adv. Sci. Technol. **95**, 202–206 (2014).

[2]M. N. Kunchur, "Novel transport behavior found in the dissipative regime of superconductors," Mod. Phys. Lett. B **9**(7), 399–426 (1995).

[3]M. González, S. Vidal, J. Viña, M. R. Osorio, J. Maza, and F. Vidal, "Electric field versus current density curves in melt-textured samples of $YBa_2Cu_3O_{7-\delta}$ under currents well above the critical current," Physica C **372–376**, 1852–1854 (2002).

[4]F. Sirois, J. Coulombe, F. Roy, and B. Dutoit, "Characterization of the electrical resistance of high temperature superconductor coated conductors at high currents using ultra-fast regulated current pulses," Supercond. Sci. Technol. **23**(3), 034018 (2010).

[5]M. Therasse, M. Decroux, L. Antognazza, M. Abplanalp, and Ø. Fischer, "Electrical characteristics of DyBCO coated conductors at high current densities for fault current limiter application," Physica C **468**(21), 2191–2196 (2008).

[6]R. Pecher, M. D. McCulloch, S. J. Chapman, L. Prigozhin, and C. M. Elliott, "3D-modelling of bulk type-II superconductors using unconstrained H-formulation," in *6th European Conference on Applied Superconductivity (EUCAS 2003), Sorrento, Italy, 14–18 September 2003* (Institute of Physics Conference Series, 2003).

[7]R. Brambilla, F. Grilli, and L. Martini, "Development of an edge-element model for AC loss computation of high-temperature superconductors," Supercond. Sci. Technol. **20**(1), 16–24 (2007).

[8]F. Roy, B. Dutoit, F. Grilli, and F. Sirois, "Magneto-thermal modeling of second-generation HTS for resistive fault current limiter design purposes," IEEE Trans. Appl. Supercond. **18**(1), 29–35 (2008).

[9]J. Maza, G. Ferro, M. R. Osorio, J. A. Veira, and F. Vidal, "Analytical approach to the thermal instability of superconducting films under high current densities," Phys. Rev. B **84**(21), 214530 (2011).

[10]C. Lacroix and F. Sirois, "Concept of a current flow diverter for accelerating the normal zone propagation velocity in 2G HTS coated conductors," Supercond. Sci. Technol. **27**(3), 035003 (2014).

[11]A. Bossavit, "What do voltmeters measure?," COMPEL Int. J. Comput. Math. Electric. Electron. Eng. **27**(1), 9–16 (2008).

[12]R. H. Romer, "What do "voltmeters" measure?: Faraday's law in a multiply connected region," Am. J. Phys. **50**(12), 1089–1093 (1982).

[13]K. T. Mcdonald, Lewin's Circuit Paradox, Tech. Rep., Princeton University, 2016.

[14]N. Riva, S. Richard, F. Sirois, C. Lacroix, B. Dutoit, and F. Grilli, "Over-critical current resistivity of YBCO coated conductors through combination of pulsed current measurements and finite element analysis," IEEE Trans. Appl. Supercond. (to be published).